Global NEST Journal, Vol 27, No 6, 07119

Optimization of fuel injection timing and pressure in CI engines using waste cooking oil biodiesel with response surface methodology

Sathiskumar S.[1]* and Priyanka E.B.[2]
[1]Department of Automobile Engineering, Kongu Engineering College, Perundurai, Erode, Tamilnadu, India
[2]Department of Mechatronics Engineering, Kongu Engineering College, Perundurai, Erode, Tamilnadu, India
Received: 07/12/2024, Accepted: 28/04/2025, Available online: 05/05/2025
*to whom all correspondence should be addressed: e-mail: Sathiskumar.auto@kongu.edu
https://doi.org/10.30955/gnj.07119

Graphical abstract

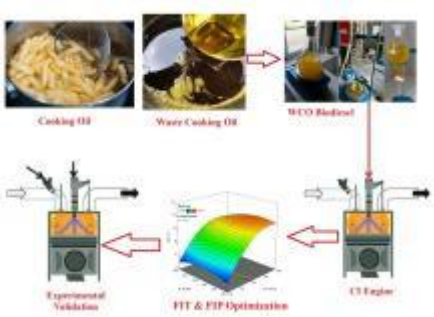

Abstract

The global automotive industry is under mounting pressure to adopt highly efficient, low-emission engine technologies due to stringent regulations and increasing environmental awareness. In response, researchers are exploring alternative fuels, such as biodiesel, to enhance energy independence and reduce emissions. Waste cooking oil (WCO) is a promising biodiesel feedstock as it addresses the food-versus-fuel debate, provides a waste management solution, and is widely available. Many countries, both developed and developing, are actively encouraging biodiesel production from WCO. This research looks at a water-cooled farm engine with one cylinder and four strokes that uses WCO instead of diesel. Using diesel and WCO at conventional injection times and pressures, preliminary testing established baseline performance. The engine was then sent through its paces with different fuel pressures (200, 350, and 500 bar) and injection timings (23°, 25°, and 27° crank angle). Experimental results revealed that variations in Fuel injection timing (FIT) and Fuel injection pressure (FIP) with WCO biodiesel significantly improved engine performance. Injection pressure of 350 bar with advanced injection time of 27° CA resulted in the greatest Brake thermal efficiency (BTE) of 31.18%. Compared to a FIP of 350 bar and FIT of 23° CA, BTE increased by 2.93% and 12.21% at FIPs of 200 bar and 500 bar, respectively, with the same FIT at maximum load. Hydrocarbon (HC) emissions were reduced by 1.29% and 6.5% at a FIP of 350 bar and 200 bar, respectively, compared to 500 bar, all with a FIT of 27° CA at maximum load. Carbon monoxide (CO) emissions also showed significant reductions of 12.2% and 5.6% at FIPs of 350 bar and 500 bar, respectively, compared to 200 bar with the same FIT at maximum load. However, nitrogen oxide (NOx) emissions increased with both advanced FIT and higher FIP under maximum load conditions. Smoke emissions decreased by 2.14% and 20.27% at FIPs of 350 bar and 500 bar, respectively, compared to 200 bar, all at a FIT of 27° CA. These findings highlight the potential of optimizing FIT and FIP to enhance performance and reduce emissions when using WCO biodiesel.

Keywords: Fuel injection timing, fuel injection pressure, waste cooking oil, response surface methodology, engine performance, emissions.

1. Introduction

The growing energy demand is driven by several factors, including an increasing global population that raises energy consumption across residential, commercial, and industrial sectors. Environmental concerns, such as the finite nature of fossil fuel reserves and their depletion, coupled with the significant contribution of fossil fuel combustion to greenhouse gas emissions and climate change, underscore the urgent need for cleaner energy alternatives to mitigate carbon footprints and ensure long-term energy security (Gültekin 2024a). As an essential means of energy generation and transportation, internal combustion (IC) engines have been important in the industrialization and development of today's civilization. Despite this, the exhaust fumes from these engines pose a significant threat to the environment since they contribute to climate change, air pollution, and respiratory illnesses (Yaashikaa *et al.* 2022). Professionals have investigated several fuel and engine modification strategies to mitigate these adverse effects. Transesterification, which produces biodiesel from animal fats, algal oil, and edible and inedible oils, is one potential method. Given its global availability, WCO has a lot of potential since it provides a workable

answer to the waste management problem and settles the food vs. fuel debate. The generation of biodiesel from WCO is being aggressively promoted by several developed and developing countries (Naik *et al.* 2022).

(Nirmala *et al.* 2020) investigated the efficiency of a diesel engine running on a combination of WCO biodiesel and conventional diesel fuel. The transesterification technique was used to create the WCO methyl ester. To determine how various fuel mixes comprising WCO methyl ester and regular diesel affected the engine's performance, they conducted experiments. Applying pure biodiesel (B100) under varying loads resulted in an 8% increase in Brake specific energy consumption (BSEC), a 15% increase in engine smoke opacity, a 10% drop in NO_x emissions, a small decrease in CO emissions, and a 15% reduction in HC, according to the results. The ideal blending ratio, according to them, for better engine performance and emissions, is anywhere between 30 and 50 percent.

Geng (Li *et al.* 2020) conducted on the combustion and NOx emissions of a six-cylinder turbocharged diesel engine found that when used in conjunction with WCO biodiesel, the engine's peak cylinder pressure and heat release rates were somewhat lower than when using pure diesel. Compared to plain diesel, the NOx emissions were reduced while using WCO biodiesel. As the percentage of biodiesel in the test fuels grew, the researchers noticed a little drop in cylinder pressure. Biodiesel also resulted in longer ignition delay (ID) and combustion duration (CD). While the peak heat release rate climbed to a maximum of 21.3% under high load, it reduced by about 14.3% under low load. Researchers found that as biodiesel percentage increased, exhaust gas temperature and NOx emissions decreased. Overall, they concluded that WCO biodiesel could be blended with conventional fuel, offering performance close to diesel without engine modifications.

(Ganesan, Viswanathan*, et al.* 2022) investigated how WCO biodiesel affected diesel engine combustion, uncontrolled gaseous emissions, and PM emissions. Fuels tested included diesel, B20, B50, B75, and pure biodiesel. The use of biodiesel led to a decrease in the maximum heat release rate, an increase in in-cylinder pressure, a shorter ID, and a shorter CD. Although biodiesel increased Brake specific fuel consumption (BSFC), it had no discernible effect on BTE across the board. The study also found that WCO biodiesel reduced particulate mass concentration and decreased particle size. Overall, the impact of biodiesel on emissions was directly related to its content in the fuel blend.

(Sathish Kumar *et al.* 2022) studied the possibility of fuelling a single-cylinder farm diesel engine with emulsified WCO. Combining water, ethanol (as a co-surfactant), and Span 80 (as a surfactant) allowed them to construct the emulsions. After considering stability, the ideal emulsion was determined to be 70% WCO, 15% water, 10% ethanol, and 5% Span 80. This mixture was then tested in the engine. In comparison to pure WCO, the WCO emulsion significantly reduced smoke and NOx emissions in performance tests conducted under varied loads. Furthermore, the emulsified gasoline reduced emissions of HC and CO. In comparison to clean WCO, the emulsified gasoline demonstrated greater in-cylinder pressure and heat release rates, according to the research. However, part-load efficiency with emulsified WCO was found to be lower.

(Kumar *et al.* 2020) investigated the effects of several mixes of WCO biodiesel on a single-cylinder farm diesel engine running at 1500 rpm with different loads. The findings demonstrated that WCO biodiesel exhibited diesel-like properties, but with a little lower BTE under all tested load scenarios. In addition, the researchers found that for low and medium engine loads, the smoke emissions from WCO biodiesel and its blends were 24% higher than diesel. This was because the biodiesel had a greater viscosity, which caused poor atomization and locally rich mixes during part-load operations.

(Gültekin 2024b) The hydrogen-diesel dual fuel (HDDF) mode is emerging as a promising alternative fuel strategy for compression ignition engines. To maximize its benefits, optimizing ECU-controlled fuel system settings is essential. Experiments were conducted at a constant speed of 1850 rpm and a 5 Nm load, with varying hydrogen ratios (11–20%) and injection timings (20–60°CA aTDC). Results showed an 8.4% reduction in specific energy consumption, a 68.4% decrease in NOx emissions, and a 16.6% rise in mechanical vibrations at a 14% hydrogen ratio and 30°CA aTDC injection timing.

(Gültekin & Ciniviz 2023)As hybrid and electric vehicles gain popularity, internal combustion engines are expected to remain widely used due to ongoing challenges with battery technology and charging infrastructure. Enhancing their performance and reducing emissions through alternative fuels is therefore essential. This study investigates the hydrogen-diesel dual fuel mode in a single-cylinder compression ignition engine equipped with a common rail injection system and an electronically controlled gas fuel system (Gültekin & Ciniviz 2024). Experiments were conducted at a constant speed of 1850 rpm with varying loads (3–9 Nm) and hydrogen injector opening times (1.6–2.0 ms). Findings indicate that higher loads increased in-cylinder pressure while reducing specific energy consumption. Emission analysis showed a rise in NO emissions but a significant decline in other pollutants. However, hydrogen energy ratios exceeding 14% had a negative impact on both performance and emissions.

(Kumar *et al.* 2024) assumed that, with the optimization of four input parameters, plastic pyrolysis oil (PPO) might compete with petroleum diesel in CI engines in terms of performance and emissions. Using RSM and a central composite rotating architecture, they assessed variables like injection time, nanoparticle concentration, compression ratio, and the fuel mix (PPO and diesel). The most efficient engine settings were determined by the regression study to be an injection timing of 20.95° bTDC, a compression ratio of 18.06, a concentration of 53.53 ppm of Al_2O_3 nanoparticles, and a blend ratio of 16.56% PPO. With errors around 5%, these ideal inputs were confirmed by real engine testing, indicating good performance. This research highlights the important factors for optimized engine performance, combustion characteristics, and

decreased emissions. It suggests that diesel engines may benefit from using PPO with Al_2O_3 nanoparticles as a fuel.

(Kumar & Pal 2022) conducted tests using a common rail direct-injection (CRDI) diesel engine that combined WCO with waste plastic oil (WPO) biodiesel plus diesel. In their experiment, they used a central composite design and ran RSM on several replies. Based on the analysis of variance (ANOVA) findings, there is a high relationship between the experimental and anticipated outputs. The R^2 values for BTE, EGT, BSFC, HC, CO, and NO_x are 98.41%, 97.02%, 99.29%, 98.49%, and 98.21%, respectively. We found that 14% biodiesel, 35% engine load, 25° bTDC FIT, and 6% EGR were the best input settings. With a BTE of 20.3%, EGT of 485.6 K, BSFC of 370.9 g/kWh, HC at 0.18 vol.%, CO at 17.8 ppm, and NO_x at 336.33 ppm, the ideal output values were obtained. These values were found to be within an acceptable range according to validation testing.

(Bragadeshwaran *et al.* 2023) examined the possibility of lowering CI engine smoke and NO_x emissions by the coordinated modification of fuel and design factors. To build an L18 orthogonal array test matrix, they chose four fuel factors and four design factors, all of which had three levels. Over the course of 18 experiments, researchers measured reactions like NO_x, smoke, and BSFC while experimenting with different combinations of these elements. To determine the importance and how the components interacted, analysis of variance was carried out. The ideal concentrations of these components for reducing BSFC, NO_x, and smoke emissions were determined by using RSM in conjunction with a desirability function. Reducing emissions while retaining engine performance was achieved via a combination of fuel and design tweaks, as both smoke and NO_x emissions reduced under these ideal circumstances without affecting BSFC.

Table 1. Literature summary of different biodiesel fuels

Fuel type	Combustion type and Comparison	Engine Type	Combustion	Performance	Emission	Ref
Millettia pinnata (B100)	Compression Ignition & Diesel	4-Stroke, 1 Cyl, DI, 1500 rpm, 5kW	↑CP, ↓ID & CD	↓BSFC ↑BTE 34.6%	↓NOx ↑CO, HC	(Kalsi & Subramanian 2017)
CSO Blends (B10 to B30)	Compression Ignition & Diesel	4-Stroke, 1 Cyl, DI, 2300 rpm, 5.5kW, CR - 18	-	↓BSFC 27% ↑BTE 36%	↓NOx 24% ↑HC, CO2-17%	(Charitha et al. 2019)
Diesel & Methane	Compression Ignition & Diesel	4-Stroke, 1 Cyl, DI, 1500 rpm, 5kW, CR – 12-19	↑CP	↓BSEC ↑BTE	↓NOx ↑CO, HC	(Armin & Gholinia 2022)
CSO biodiesel	Compression Ignition & Diesel	4-Stroke, 1 Cyl, DI, 1500 rpm, 5.4kW, CR – 17.5	↓CP 5.1%, ↓HRR 3.7%	↓BSFC ↓BSFC	↓NOx 42.7% ↑CO 11.4% ↑HC 4.5%	(Ganesan, Le, et al. 2022)
Diesel & Isobutanol	Compression Ignition & Diesel	4-Stroke, 1 Cyl, DI, 1500 rpm, 4.4kW, CR – 17.5, FIP – 220 bar	↓CP 4.3% ↓HRR 4.1%	↓BSFC 4.3% ↑BTE 3.5%	↓NOx 57.5% ↑CO 13.1% ↑HC 6.5%	(Ganesh et al. 2019)
WCO biodiesel & Ethanol	Compression Ignition & Diesel	4-Stroke, 1 Cyl, DI, 1500 rpm, 3.7kW, CR – 16, FIP – 200 bar	↓CP 3.1% ↓HRR 4.7%	↓BSFC ↑BTE 6%	↓NOx% ↑CO 13.4% ↑HC 8.5%	(Guan et al. 2017)
WCO Biodiesel & LPG	Compression Ignition & Diesel	4-Stroke, 4 Cyl, DI, 3200 rpm, CR – 19	↑CP 11.6% ↑HRR 38.8%	↓BSFC ↑BTE 1.5%	↓NOx 1.9% ↑CO 44.9% ↑HC 24.7%	(Kumar et al. 2019)

Table 1 shows the summary of literature review, it indicates that vegetable oils, particularly WCO, can serve as a fuel source for diesel engines for limited durations without significant issues. The increased emissions and decreased thermal efficiency caused by WCO's higher viscosity and density when used directly as a substitute fuel in diesel engines are the outcomes of this comparison. Researchers have previously explored blending, transesterification, and emulsification of WCOs as practical and effective methods for fuel modification. Some studies suggested adjusting FIT and FIP to control emissions and optimize performance. But very few studies have investigated the effect of FIT and FIP on WCO biodiesel blends.

The novelty of this work is using (B100) WCO biodiesel in dual fuel engine with different FIT and FIP. The main purpose of this study is to assess the qualities and optimize the input parameters for using WCO biodiesel in the test engine with varying loads. This study looks at the possibility of substituting WCO biodiesel for diesel in four-stroke, single-cylinder CI engines, which are often used in farming. WCO collected from the institute's hotels and restaurants is used for this evaluation of engine performance. First phase, tests were conducted using diesel and WCO with conventional injection timings, pressures, and varying engine load to gather baseline data. In phase two, the engine was put through its paces using a range of fuel pressures (200, 350, and 500 bar) and injection timings

(23°CA, 25°CA, and 27°CA). Optimal operating conditions were determined using the RSM and then evaluated with actual experimental testing.

Table 2. Fuel's physical and chemical characteristics

Property	Diesel (Mean ± SD)	WCO Biodiesel (Mean ± SD)
μ - Kinematic Viscosity (cSt) @ 40° C	2.417 ± 0.03	4.027 ± 0.05
ρ - Density (kg/m^3) @27° C	828.1 ± 1.2	866.0 ± 1.5
LHV - Lowest heating value (MJ/kg)	42.11 ± 0.1	38.034 ± 0.08
CI - Cetane Index	56 ± 0.5	66 ± 0.6
ON - Octane number	--	-
LHoV - Enthalpy of vaporization (kJ/kg)	251 ± 2	328 ± 2.5
SIT - Self ignition temperature (° C)	211 ± 1	-
φ - Air/Fuel ratio	14.4 ± 0.1	-
C - Carbon	85.74 ± 0.5	76.26 ± 0.4
H_2 - Hydrogen	13.72 ± 0.2	13.308 ± 0.2
O_2 - Oxygen	-	9.819 ± 0.3

Table 3. Analysis of uncertainty

Parameters	Percentage of Uncertainty
Engine speed	±0.54
Load	±2.24
Brake power	±2.67
Total fuel consumption	±1.26
Brake thermal efficiency	±1.319
Brake-specific fuel consumption	±2.323
In-cylinder pressure	±1.75
Carbon dioxide	±1.8
Carbon monoxide	±1.4
Hydrocarbon	±3.2
Nitric oxide	±2.6
Smoke emission	±1.4

Table 4. Specifications of experimental test engine and exhaust measurements

Make/model	Kirloskar TV-1
Engine capacity	661.45 cm3
Type	Single cylinder, vertical, direct injection, 4-stroke, constant speed, water cooled, diesel engine
Ignition	Compression ignition
Cylinder bore and stroke length	87.5 mm X 110 mm
Compression ratio	17.5:1
Rated power	3.50 kW @ 1500 rpm
Fuel injection timing	23°bTDC
Dynamometer type	Eddy current with water cooled
Injection pressure	210 bar
Smoke meter: (Make & Model - AVL 437 smoke meter)	To measure Smoke Opacity, Range 0–100%, Accuracy: ±1%
Gas Analyser: (Make & Model - AVL 444 di-gas analyser)	To measure CO, NOx, CO_2 and HC emissions
	CO - Range: 0–10% volume, Accuracy: 0.01% volume
	CO_2 - Range: 0–20% volume, Accuracy: 0.1% volume
	HC - Range: 0–20,000 ppm, Accuracy: 1 ppm
	NOx - Range: 0–5000 ppm, Accuracy: 1 ppm

2. Methodology and materials

2.1. WCOME biodiesel preparation

The primary sources of waste cooking oil (WCO) for biodiesel generation are the institute's hostel, as well as nearby hotels and restaurants. A two-way round-bottom flask is used to carry out the acid esterification and alkali transesterification reactions. A water-cooled condenser stops the methanol from evaporating while the magnetic stirrer with a heater keeps the mixture from scorching. A basin filled with water is used to partly submerge the round-bottom flask so that it may be heated uniformly. There are controls for the water temperature and the speed of the stirrer in this setup. The condenser is constantly cooled by an external water supply to reduce the temperature of the methanol that has been evaporated from the oil. Catalysts, such as KOH and anhydrous H_2SO4, are added to facilitate the chemical reaction. For

transesterification, 1000 mL of WCO is taken in a two-way flask. Catalyst solution wear prepared with a beaker, 2.5 g of NaOH pellets and 200 mL of CH_3OH methanol is combined. Then methanol and NaOH are mixed until the NaOH is completely dissolved. Further combining the catalyst and oil resulting solution is added to the WCO in the two-way flask and properly mixed, and it is (methoxide solution and WCO) heated to 60°C–65°C and continuously stirred at a constant speed for 1 hour. After transferring the solution to a separatory container, it is let to settle for 24 hours. Glycerin settles at the bottom, and methyl ester (coarse biodiesel) forms the top layer. Glycerin and the methyl ester are separated. To get rid of any raw methanol, the coarse biodiesel is heated to above 100°C for ten to fifteen minutes. Remaining contaminants, such as sodium hydroxide, are eliminated by washing the biodiesel with 350 mL of water per 1000 mL of biodiesel. The purified biodiesel, a methyl ester of WCO, is obtained and subjected to performance, emission, and combustion tests in a diesel engine. **Table 2** contained a list of the fuel attributes (Sathiskumar & Priyanka 2024).

2.2. Uncertainty

Numerous functional and physical variables contribute to minor uncertainties during measurement. Despite careful experimentation, the measured values may deviate slightly from the true values, leading to the possibility of errors. To address this, a comprehensive error assessment was conducted through uncertainty analysis. The root mean square method was employed for this analysis. **Table 3** presents the uncertainty analysis of the parameters related to the experiment (Tamilvanan *et al.* 2020).

The total percentage uncertainty for the experiment is calculated as

$$= \sqrt{\begin{matrix}1.0^2+1.0^2+1.2^2+0.8^2+0.7^2 \\ +0.7^2+0.8^2+1.1^2+1.0^2\end{matrix}} = 2.81\%$$

Figure 1 and **Table 4** show how the engine test setup is arranged artistically. Using an eddy current dynamometer, the given engine test rig can run at different loads from 0% to 100%. The inlet manifold air flow rate in the supply line is also measured by using an anemometer. Fuel rate of flow calculations were made using the burette designs. The five gas emissions were measured using the AVL gas analyzer (Version: 444 di-gas). The amount of smoke opacity is measured using a smoke meter of the AVL 437C type. A Piezo sensor fixed on the top of the cylinder head, was used to measure the pressure inside the cylinder. The sensor's signal was processed into a digital signal by a charging amp, which was subsequently gathered and examined with a combustion flame analyzer. Using an AVL crank angle sensor, pressure information of 100 consistent continuous cycle was collected at a precision of 0.2 CAD for each operating point. The studies were carried out with different weights while the engine speed at 1500 rpm. Running the engine on diesel fuel first, then on WCO biodiesel, brought about stable working conditions. Each experiment was repeated three times to ensure consistent performance, combustion, and emission readings, with the average values used for analysis. In the first phase, baseline data was generated by testing the engine with WCO as fuel. The tests were carried out using a range of different engine loads and utilizing normal injection times and pressures. The study evaluated the test engine through varying FIP (200, 350, and 500 bar) and FIT (23, 25, and 27° CA). The most effective operational parameters for a FIT and FIP approach were determined using RSM (Tamilvanan *et al.* 2023).

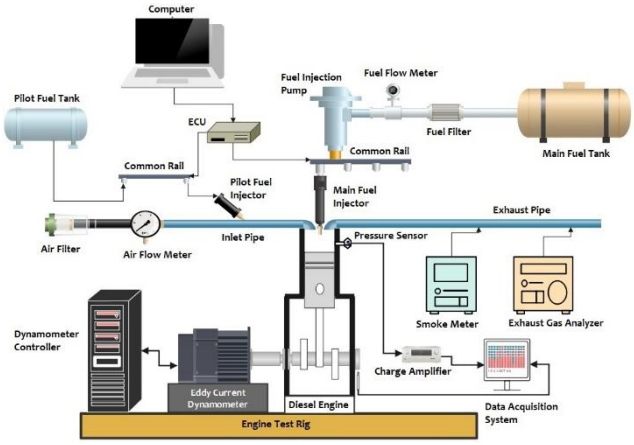

Figure 1. Experimental setup

Table 5. Degrees of engine input

Description	Design parameters		
	A: Load	B: FIP	C: FIT
Units	%	bar	CA
Levels	20 – 100	200-500	21 - 25
Intervals	5	3	3

2.3. Response Surface Methodology Analysis

The experimental design parameters and their levels, as summarized in **Table 5** were established using the split-plot approach, which was informed by the results of a prior investigation. A customized split-plot analysis was used to evaluate the importance of the linear and non-linear quadratic models that were built. After that, we ran an analysis of variance (ANOVA) to see how the design factors affected the answers. Three separate tests were used to determine if the model was adequate. To begin, we looked at the design factors' effects on the response using the F-value and p-value; a larger F-value and smaller p-value suggest that the parameter had a greater effect. The second step was to examine the accuracy of the projected outcomes using a R^2 test. A precision of 0.90 or above indicated a significant alignment between the experimental and predicted values, while a R^2 value between 0 and 1 was considered adequate. The last step was to run a lack-of-fit test; a non-significant result indicated that the model had been well-fitted (Sathiskumar & Priyanka 2024). Initial optimization research looked at how three important design variables—Load, FIT, and FIP—impacted ID, CD, BTE, BSFC, HC, CO, NOx, and smoke emissions, among other performance and emission metrics. From 20% to 100% load, from 23°CA to 27°CA, and from 200 bar to 500 bar, respectively, are the ranges for FIT, FIP, and Load. The goal was to find a sweet spot for FIT and FIP settings that would allow the engine to run

efficiently while still limiting emissions; this would provide useful information for improving engine performance with less of an effect on the environment. **Table 6** summarizes the results of calculating the response variables using well-established equations based on experimental data.

$$ID(CA) = +14.24 - 1.98 \times A - 1.00 \times B - 0.9500 \times C - 0.0167 \times AB - 0.0167 \times AC + 0.012 \times BC + 0.0952 \times A^2 - 0.0333 \times B^2 - 0.0833 \times C^2 \quad (1)$$

$$CD(CA) = +70.83 + 4.43 \times A - 2.58 \times B - 2.57 \times C + 0.2140 \times AB + 0.1333 \times AC - 0.6750 \times BC - 0.4286 \times A^2 - 0.7167 \times B^2 + 0.033 \times C^2 \quad (2)$$

$$BTE(\%) = +27.29 + 7.26 \times A - 0.6998 \times B + 0.8875 \times C - 0.5095 \times AB + 0.5682 \times AC - 0.0912 \times BC - 5.14 \times A^2 - 1.71 \times B^2 + 0.1445 \times C^2 \quad (3)$$

$$BSFC(kg/kWh) = 0.3332 - 0.1648 \times A + 0.0110 \times B - 0.0147 \times C + 0.0029 \times AB + 0.0002 \times AC + 0.0008 \times BC + 0.1595 \times A^2 + 0.0318 \times B^2 - 0.0025 \times C^2 \quad (4)$$

$$HC(g/kWh) = +4.09 - 6.16 \times A + 0.2635 \times B - 0.3210 \times C - 0.1344 \times AB + 0.2907 \times AC - 0.0400 \times BC + 4.88 \times A^2 - 0.1279 \times B^2 + 0.1241 \times C^2 \quad (5)$$

$$CO(g/kWh) = +20.61 - 37.12 \times A - 2.24 \times B - 2.23 \times C + 2.23 \times AB + 2.46 \times AC + 0.2072 \times BC + 31.13 \times A^2 + 0.2618 \times B^2 + 0.8235 \times C^2 \quad (6)$$

$$NO_X(g/kWh) = +9.37 - 1.80 \times A + 0.777 \times B + 0.6635 \times C - 0.1087 \times AB - 0.0922 \times AC - 0.0678 \times BC + 0.5443 \times A^2 + 0.1662 \times B^2 - 0.1021 \times C^2 \quad (7)$$

$$Smoke\ opacity(\%) = +15.62 + 5.75 \times A - 1.17 \times B - 1.51 \times C - 0.4064 \times AB - 0.6890 \times AC - 0.0198 \times BC - 0.7607 \times A^2 + 0.5301 \times B^2 + 0.1259 \times C^2 \quad (8)$$

Table 7 contains the p-values that were used to pick the models for each outcome. Models with p-values below 0.0001 were considered statistically significant, reflecting a confidence level of 95%. As indicated in **Table 7**, all selected models were well-suited for predicting responses, meeting the criterion of $p < 0.0001$. To determine whether design elements had a substantial impact on the results, we used analysis of variance (ANOVA) to assess their relative importance. Then, we ran regression analysis to see how each design parameter, alone and in combination, affected the outcomes. Equations 1-8 offer the polynomial equations that reflect the response factors that are significant and those that are significant (Li *et al.* 2019).

The modified version of the regression coefficient (R^2) was used to evaluate the model's capacity to forecast outcomes from experimental data. R^2 measures the fit of the model and increases as more independent variables are added, with values ranging from 0 to 1. An R^2 and adjusted R^2 above 0.9 signify high predictive accuracy. The adjusted R^2 is improved by lowering the number of inconsequential characteristics, and experimental dependability is shown by a difference between R^2 and adjusted R^2 of less than 0.2. As shown in **Table 8**, the R^2 values for all findings range from 0.9688 to 0.9957, exceeding the 0.9 benchmark and confirming strong model precision. Notably, the F-values for FIT and FIP in parameters like ID, CD, BTE, BSFC, HC, CO, NOx, and smoke emissions are higher than those for Load, with all associated p-values below 0.05, indicating that FIT and FIP have a greater influence on these outcomes. However, for BTE, the F-value for Load surpasses that of FIT and FIP, with p-values below 0.05, highlighting the significant impact of Load on BTE (Dey *et al.* 2021).

3. Results and discussion

3.1. Performance characteristics of FIP and FIP

3.1.1. ID of different FIT and FIP

Figure 2 illustrates the variation in ID for WCO biofuel across different engine load conditions as influenced by injection pressure and timing. As injection pressures and timings are fine-tuned, the ID steadily drops. For injection pressures of 200 bar, 350 bar, and 500 bar, the conventional injection time was 23°CA, and the corresponding IDs were 14°, 13°, and 12° CA. With an advanced injection time of 27°CA and 500 bar, the shortest ID was measured to be 10.5°CA. Improving the injection time and pressure improved the WCO biofuel's combustion efficiency, which decreased ID. Under these circumstances, the ID dropped from 18°CA to 10.5°CA. Compared to static injection conditions, the ID was lowered to 14.61°CA with an improved injection timing of 23°CA bTDC and an injection pressure of 350 bar. Additional improvements brought it down to 10.5°CA. The reduction is caused by the fact that fuel droplets are finer-atomized at higher pressures, leading to an increase in fuel accumulation throughout the ID period (Hirkude & Padalkar 2014). Additionally, smaller droplet sizes, shorter breakup lengths, and improved dispersion contribute to a shorter ID. These factors collectively extend the premixed combustion phase, allowing a greater portion of the fuel to burn more efficiently (Puhan *et al.* 2009).

3.1.2. CD of different FIT and FIP

Figure 3 shows that CD changes for WCO biofuel under various engine load circumstances as a function of injection pressure and time. Across all load levels, the CD for WCO biofuel reduces steadily as injection pressure and time advance. The CD was recorded as 78°, 76.5°, and 75° CA at injection pressures of 200 bar, 350 bar, and 500 bar, respectively, at the normal injection time of 23°CA. Injection pressure of 500 bar with advanced injection time of 27°CA resulted in the lowest CD measured at 68.5°CA. By increasing the injection pressure and adjusting the time, the combustion process is improved, leading to a decrease in CD. These adjustments lead to a decrease in CD from 78°CA to 68.5°CA. The premixed combustion phase is accelerated by higher injection pressures, and the diffusion combustion phase is improved by the increasing oxygen concentration of WCO biofuel. These combined effects contribute to a more efficient combustion process and shorter CD (Prabu *et al.* 2017).

3.1.3. BTE of different FIT and FIP

Figure 4 shows the relationship between engine load conditions, injection pressures, and timings as they relate

to BTE for WCO biofuel. Regardless of the injection timing (23°, 25°, or 27° CA bTDC) that was examined, the BTE grew as the injection pressure went from 200 bar to 350 bar. However, under all load situations, BTE decreased when injection pressure was increased to 500 bar. Higher injection pressures (up to 350 bar) increase BTE because they lead to more efficient combustion via better fuel atomization and fuel-air mixing. At these pressures, the fuel droplet size decreases significantly, enabling better mixing with air during the ID, thereby enhancing combustion (Agarwal *et al.* 2015). Conversely, the reduction in BTE at 500 bar occurs due to excessively small fuel droplet sizes that lose momentum, resulting in poor fuel-air distribution. Inadequate air entrainment and combustion result from this and the lower relative velocities of the fuel particles (Sharma & Murugan 2017). The studies were conducted to determine the most effective injection time and pressure by observing the maximum BTE. At maximum engine load, the BTE peaked at 27.91% with an injection pressure of 350 bar and a timing of 23° CA.

3.1.4. BSFC of different FIT and FIP

Figure 5 illustrates the BSFC of WCO biofuel under varying injection pressures and timings across different engine load conditions. Because combustion efficiency improves with increasing engine load, the data shows that BSFC drops with increasing engine load. Different injection timings (23°CA, 25°CA, and 27°CA) and pressures (200 bar, 350 bar, and 500 bar) were used to record BSFC values at full load; the corresponding measurements were about 0.344, 0.326, 0.307, 0.334, 0.315, 0.304, 0.380, 0.349, and 0.339 kg/kWh. There was a slight decrease in BSFC for all three injection timings (23°, 25°, and 27°CA bTDC) as the injection pressure went from 200 bar to 350 bar. Furthermore, under all load situations, BSFC values were reduced when the injection pressure was raised to 350 bar. The improvement in combustion efficiency and increased atomization led to greater BTE and this decrease, especially at 27°CA bTDC and 350 bar. In contrast, lower injection pressures, such as 200 bar at 23°CA bTDC, showed a noticeable increase in BSFC at lower engine loads due to suboptimal atomization characteristics of the WCO biodiesel (Akash *et al.* 2017).

3.2. Emission characteristics of FIP and FIP

3.2.1. HC emission of different FIT and FIP

The main causes of HC emissions in diesel engine exhaust are low temperatures inside the cylinder, flame quenching, inadequate fuel evaporation, fuel trapped in crack areas, and very lean mixes (Li *et al.* 2019). The graph in **Figure 6** shows how the HC emissions from WCO biofuel changed when the injection pressures and timings were changed under different engine load circumstances. Injection pressures of 200, 350, and 500 bar were found to produce HC emissions of 2.28, 2.53, and 2.56 g/kWh for WCO biofuel at full engine load and typical injection time of 23°CA, respectively. Due to better combustion and smaller fuel droplet sizes, HC emissions are reduced at higher injection pressures. However, when injection pressure increases further, the droplets become finer and are injected at higher velocities. This can result in greater HC emissions, as the high-speed droplets collide with cylinder walls, creating regions with incomplete combustion. Consequently, higher FIP generally lead to increased HC emissions across all engine loads (Maurya & Agarwal 2014). On the other hand, advancing the injection timing slightly reduces HC emissions for all injection pressure levels. At elevated injection pressures, finer fuel droplets are formed, which may reach the cylinder walls at very high velocities. This interaction causes a cooling effect in the combustion zone near the cylinder walls, contributing to higher HC emissions (Kannan & Anand 2012). The primary reason for the decrease in HC emissions while using advanced injection time is the shorter ID. The effect of injection time on HC production is negligible in CI engines since they run on a low air-fuel combination (Arunprasad & Balusamy 2018).

3.2.2. CO emission of different FIT and FIP

In **Figure 7**, we can see how the CO emissions from WCO biofuel fluctuate as a function of engine load, injection pressure, and injection time. A reduction in CO emissions was seen across all loads when the injection pressure was increased. The CO emissions measured at standard injection timing of 23°CA bTDC were 13.32 g/kWh for 200 bar, 12.47 g/kWh for 350 bar, and 11.77 g/kWh for 500 bar. Smaller fuel droplets created at greater pressures improve fuel-air mixing, which in turn leads to more efficient combustion, and this is the main cause of the decrease. Also, CO emissions were significantly decreased across all loads when the injection time was advanced (Ashok *et al.* 2017). Compared to 25°CA and 23°CA bTDC, CO emissions were much lower at 27°CA. The longer physical delay brought about by advanced timing is responsible for this enhancement; it leads to greater fuel-air mixing and more efficient oxidation of carbon particles in the fuel. As a result, combustion becomes more efficient, reducing CO emissions (Wang *et al.* 2020).

3.2.3. NOx emission of different FIT and FIP

With different injection timings (23°CA, 25°CA, and 27°CA) and pressures (200 bar, 350 bar, and 500 bar), NOx emissions were measured at peak load and were about 7.07, 7.87, 7.98, 7.34, 8.06, 8.85, 8.34, 9.09, and 9.43 g/kWh, respectively. In **Figure 8**, we can see how the NOx emissions change under different engine load circumstances when we infuse WCO biofuel at different times and pressures. Nox emissions reach their highest point at 500 bar injection pressure and injection timings of 25°CA and 27°CA, respectively, reaching 12.64 g/kWh and 13.18 g/kWh, according to the data. An increase in injection pressure causes the premixed combustion phase to burn more intensely, which in turn causes greater in-cylinder temperatures and increased NOx emissions (Sharma & Murugan 2016). A significant rise in NOx emissions was seen at an injection pressure of 500 bar for all load circumstances and injection timings (23°CA, 25°CA, and 27°CA). The reason for this improvement is because WCO biofuel is better atomized, evaporates faster, and mixes more thoroughly, all of which contribute to a shorter chemical delay time and better combustion efficiency (Saravanan *et al.* 2020).

Table 6. Experimental Matrix

Exp. No.	A: Load (%)	C: FIP (Bar)	B: FIT (CA)	Performance characteristics				Emission characteristics			
				ID (CA)	CD (CA)	BTE (%)	BSFC (kg/kWh)	HC (g/kWh)	CO (g/kWh)	NOx (g/kWh)	Smoke (%)
1	20	200	23	18	70	13.13	0.721	16.165	106.692	9.907	11.803
2	40	200	23	17	72	21.26	0.445	7.074	45.045	8.951	14.128
3	60	200	23	16.5	75	25.72	0.368	4.418	26.215	8.026	19.137
4	80	200	23	15	76.5	27.315	0.347	2.921	18.392	7.135	23.300
5	100	200	23	14	78	27.51	0.344	2.284	13.323	7.066	24.480
6	20	200	25	17.5	68	13.26	0.714	15.339	97.288	10.985	10.730
7	40	200	25	16	71	21.05	0.450	6.252	41.513	9.891	12.843
8	60	200	25	15	73	25.88	0.366	4.105	24.033	8.827	17.302
9	80	200	25	14.5	75	28.34	0.334	2.726	16.909	7.957	21.198
10	100	200	25	13.5	76.5	29.03	0.326	2.226	13.503	7.870	22.287
11	20	200	27	16	66	13.98	0.677	14.861	93.384	11.811	10.131
12	40	200	27	15.5	68	22.52	0.420	6.136	40.183	10.139	11.938
13	60	200	27	14	70.5	27.25	0.347	4.035	23.188	9.464	16.267
14	80	200	27	13	73	29.96	0.316	2.672	16.408	8.372	19.534
15	100	200	27	12.5	75	30.87	0.307	2.162	12.203	7.980	20.267
16	20	350	23	17	68	13.81	0.685	16.274	99.618	10.732	10.730
17	40	350	23	16.5	71	22.54	0.420	7.846	42.397	9.622	12.843
18	60	350	23	15	74	26.67	0.355	4.720	24.590	8.577	17.597
19	80	350	23	14.5	75.5	28.16	0.336	3.274	17.241	7.635	21.109
20	100	350	23	13	77	28.34	0.334	2.529	12.473	7.344	22.232
21	20	350	25	16	66	14.58	0.649	15.576	91.336	11.772	9.755
22	40	350	25	15.5	69	22.73	0.416	7.265	38.590	10.476	11.676
23	60	350	25	14	71	27.17	0.348	4.475	22.389	9.299	15.805
24	80	350	25	13.5	73	29.51	0.321	3.125	15.709	8.229	19.089
25	100	350	25	12	75	30.06	0.315	2.361	12.576	8.062	20.043
26	20	350	27	15.5	63	14.68	0.645	15.027	87.384	12.324	9.205
27	40	350	27	14.5	65	23.65	0.400	6.993	37.703	11.379	10.508
28	60	350	27	13	68	28.61	0.331	4.396	21.864	10.081	14.358
29	80	350	27	12	71	30.56	0.310	3.109	15.453	9.173	17.245
30	100	350	27	11.5	73	31.18	0.304	2.278	11.442	8.853	17.717
31	20	500	23	16	66	12.88	0.735	16.890	93.715	11.943	10.364
32	40	500	23	15	68.5	20.13	0.470	8.046	39.968	10.901	12.232
33	60	500	23	14	71	24.36	0.389	4.989	23.231	9.793	16.719
34	80	500	23	13.5	73.5	25.84	0.366	3.411	16.302	8.785	20.259
35	100	500	23	12	75	24.88	0.380	2.565	11.766	8.338	21.557
36	20	500	25	15.5	63	13.12	0.721	15.945	86.427	12.643	9.290

37	40	500	25	14	64.5	20.27	0.467	7.149	36.662	11.444	11.120
38	60	500	25	13.5	67	24.58	0.385	4.555	21.340	10.395	15.190
39	80	500	25	12	69	26.96	0.351	3.196	14.966	9.299	18.205
40	100	500	25	11.5	71	27.15	0.349	2.432	11.907	9.092	19.420
41	20	500	27	14.5	60	13.48	0.702	15.374	83.482	13.181	8.571
42	40	500	27	13	62.5	21.26	0.445	7.099	35.547	12.011	10.008
43	60	500	27	12	64	25.72	0.368	4.391	20.489	10.726	13.722
44	80	500	27	11	66.5	27.56	0.343	2.930	14.506	9.737	16.380
45	100	500	27	10.5	68.5	27.89	0.339	2.311	10.800	9.429	17.342

Table 7. ANOVA outcomes derived from the optimization investigation

Variables		A-Load	B-FIP	C-FIT	AB	AC	BC	A^2	B^2	C^2
ID (CA)	F	1233.13	420.33	379.35	0.0584	0.0584	0.0134	1.42	0.1557	0.973
	p	0.0001	0.0001	0.0001	0.8105	0.8105	0.0001	0.324	0.6956	0.3307
CD (CA)	F	2099.66	950.58	938.35	0.0256	1.27	43.27	6.87	24.39	0.0528
	p	0.0001	0.0001	0.0001	0.0001	0.2682	0.0001	0.0129	0.0001	0.8197
BTE (%)	F	6541.11	81	130.27	21.47	26.7	0.9181	1146.53	161.49	1.15
	p	0.0001	0.0001	0.0001	0.0001	0.0001	0.3445	0.0001	0.0001	0.2907
BSFC (kg/kWh)	F	797.88	4.76	8.46	0.1654	0.0008	0.0152	261.55	13.23	0.0797
	p	0.0001	0.036	0.0063	0.6867	0.977	0.9024	0.0001	0.0009	0.7794
HC (g/kWh)	F	1066.29	2.6	3.86	0.3384	1.58	0.04	234.64	0.2045	0.1926
	p	0.0001	0.1156	0.0573	0.5645	0.2164	0.8427	0.0001	0.6539	0.6634
CO (g/kWh)	F	944.73	4.58	4.55	2.28	2.76	0.0262	232.49	0.0209	0.2066
	p	0.0001	0.0393	0.04	0.1401	0.1056	0.8724	0.0001	0.8859	0.6522
NOx (g/kWh)	F	2247.39	559.43	407.02	5.46	3.93	2.83	71.91	8.51	3.21
	p	0.0001	0.0001	0.0001	0.0253	0.0552	0.1013	0.0001	0.0061	0.0816
Smoke (%)	F	1162.01	63.77	107	3.88	11.14	0.0123	7.13	4.4	0.248
	p	0.0001	0.0001	0.0001	0.057	0.002	0.9123	0.0114	0.0433	0.6216

Table 8. Optimized model results of FIT and FIP

Description	Std Deviation	Mean	C.V. %	R^2	Adjusted R^2	Predicted R^2	Adeq Precision
ID (CA)	0.2672	14.21	1.88	0.9831	0.9787	0.9722	62.3763
CD (CA)	0.4589	70.16	0.6542	0.9915	0.9893	0.9861	88.5942
BTE (%)	0.4259	23.68	1.8	0.9957	0.9946	0.993	90.198
BSFC (kg/kWh)	0.0277	0.4325	6.4	0.9688	0.9608	0.9492	33.3824
HC (g/kWh)	0.8945	6.53	13.7	0.974	0.9673	0.9582	33.866
CO (g/kWh)	5.73	36.89	15.53	0.9715	0.9641	0.9534	33.4528
Nox (g/kWh)	0.1801	9.68	1.86	0.9895	0.9868	0.9827	76.35
Smoke (%)	0.7995	15.68	5.1	0.9749	0.9684	0.9601	44.6873

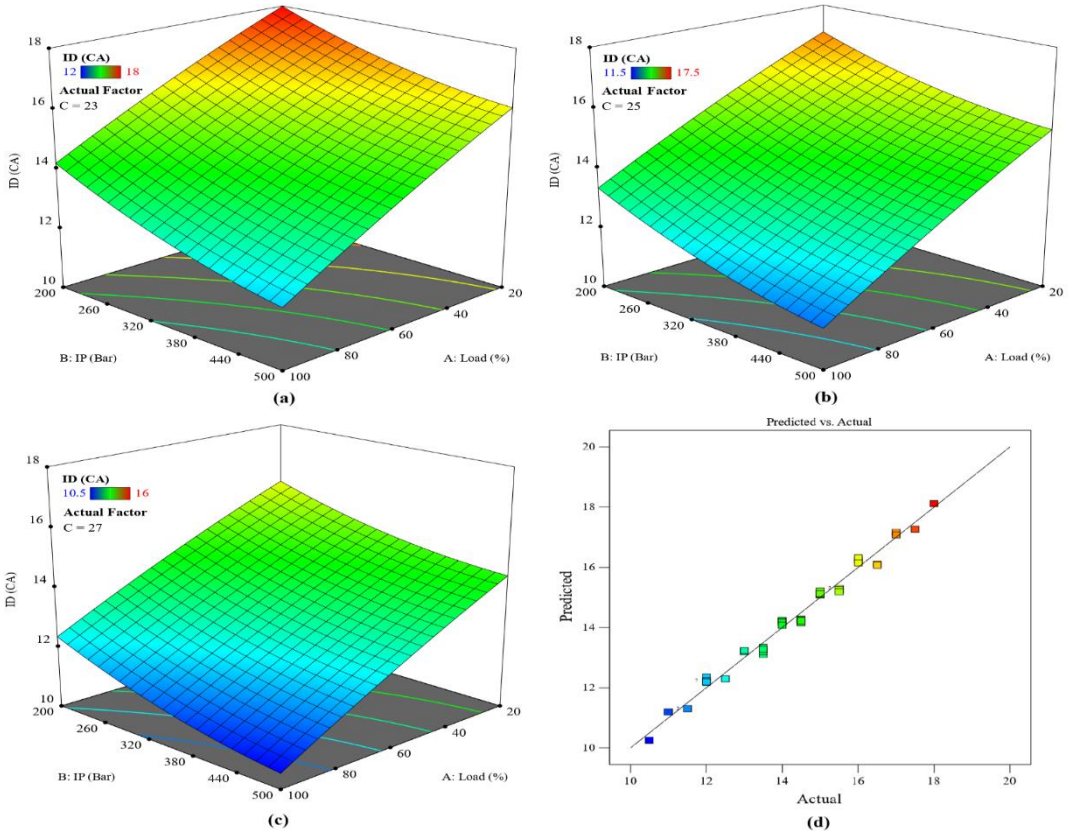

Figure 2. Effects ID with engine load for (a) FIT 23° CA (b) FIT 25° CA (c) FIT 27° CA (d) Predicted vs actual ID

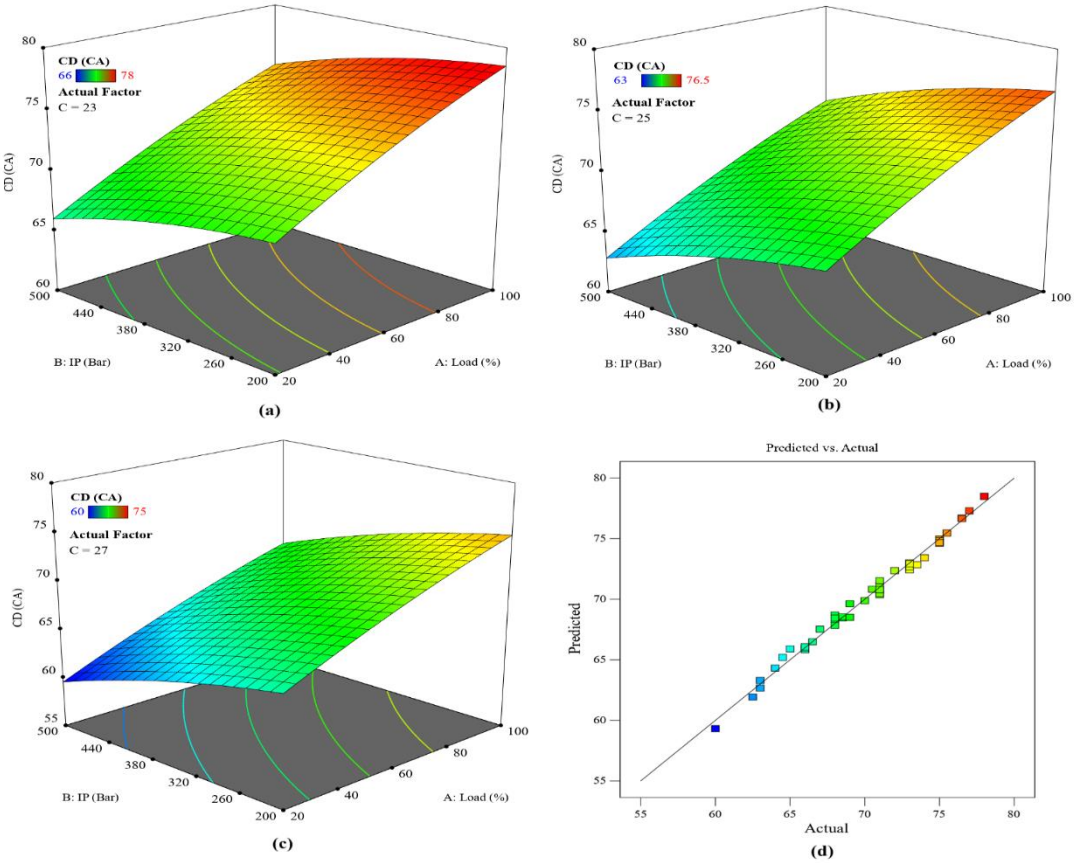

Figure 3. Effects CD with engine load for (a) FIT 23° CA (b) FIT 25° CA (c) FIT 27° CA (d) Predicted vs actual CD

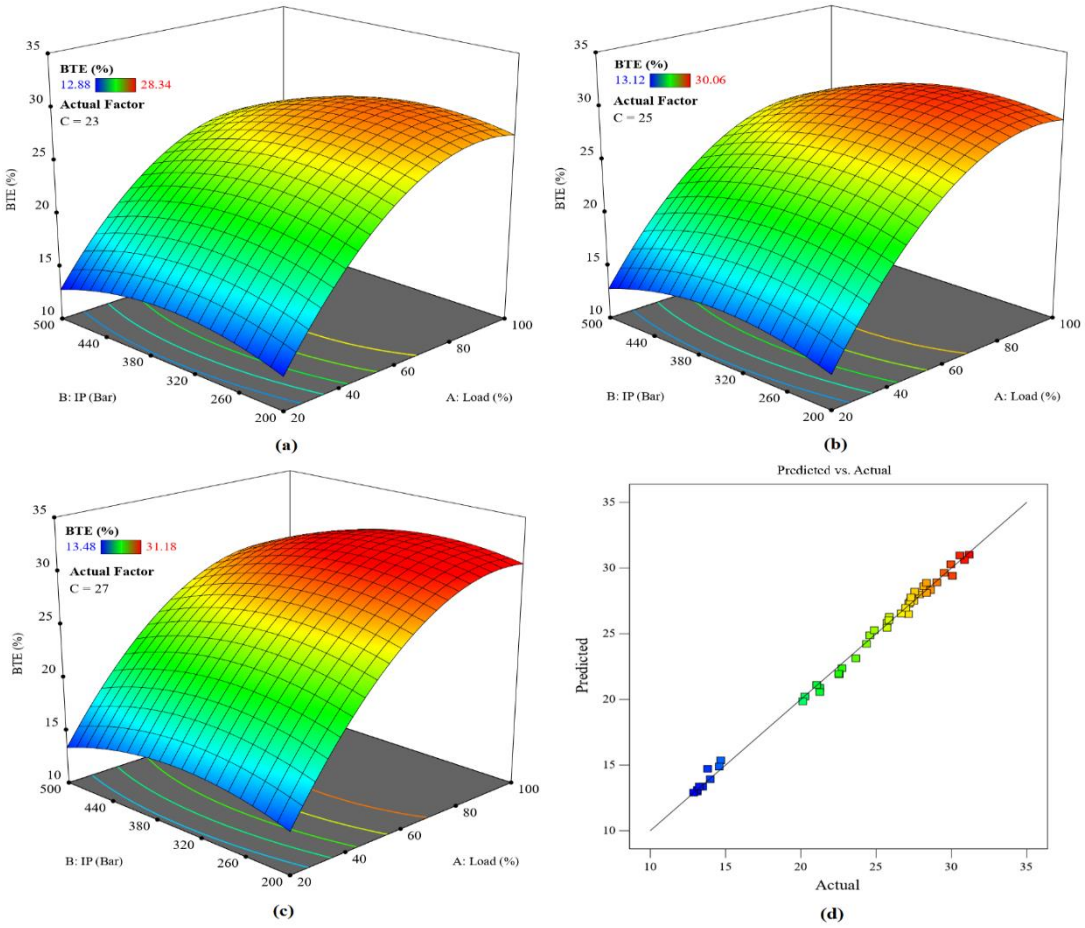

Figure 4. Effects BTE with engine load for (a) FIT 23° CA (b) FIT 25° CA (c) FIT 27° CA (d) Predicted vs actual BTE

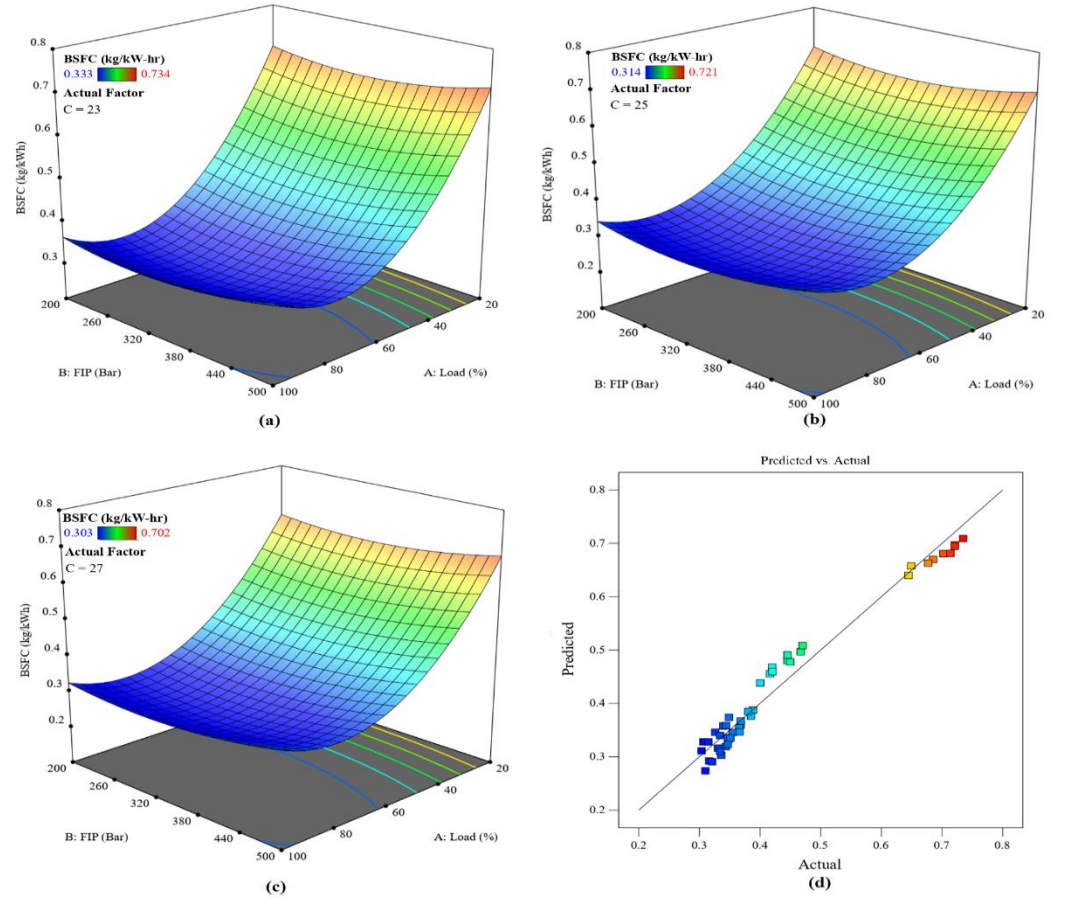

Figure 5. Effects BSFC with engine load for (a) FIT 23° CA (b) FIT 25° CA (c) FIT 27° CA (d) Predicted vs actual BSFC

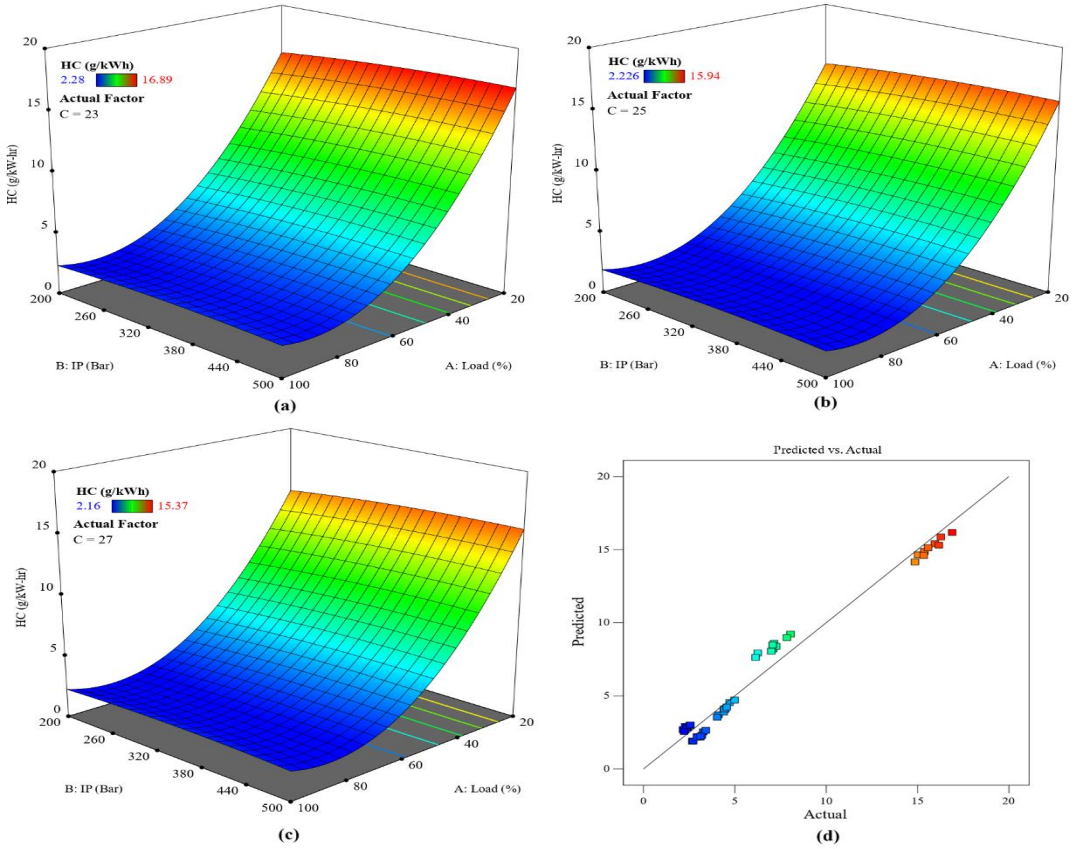

Figure 6. Effects HC with engine load for (a) FIT 23° CA (b) FIT 25° CA (c) FIT 27° CA (d) Predicted vs actual HC

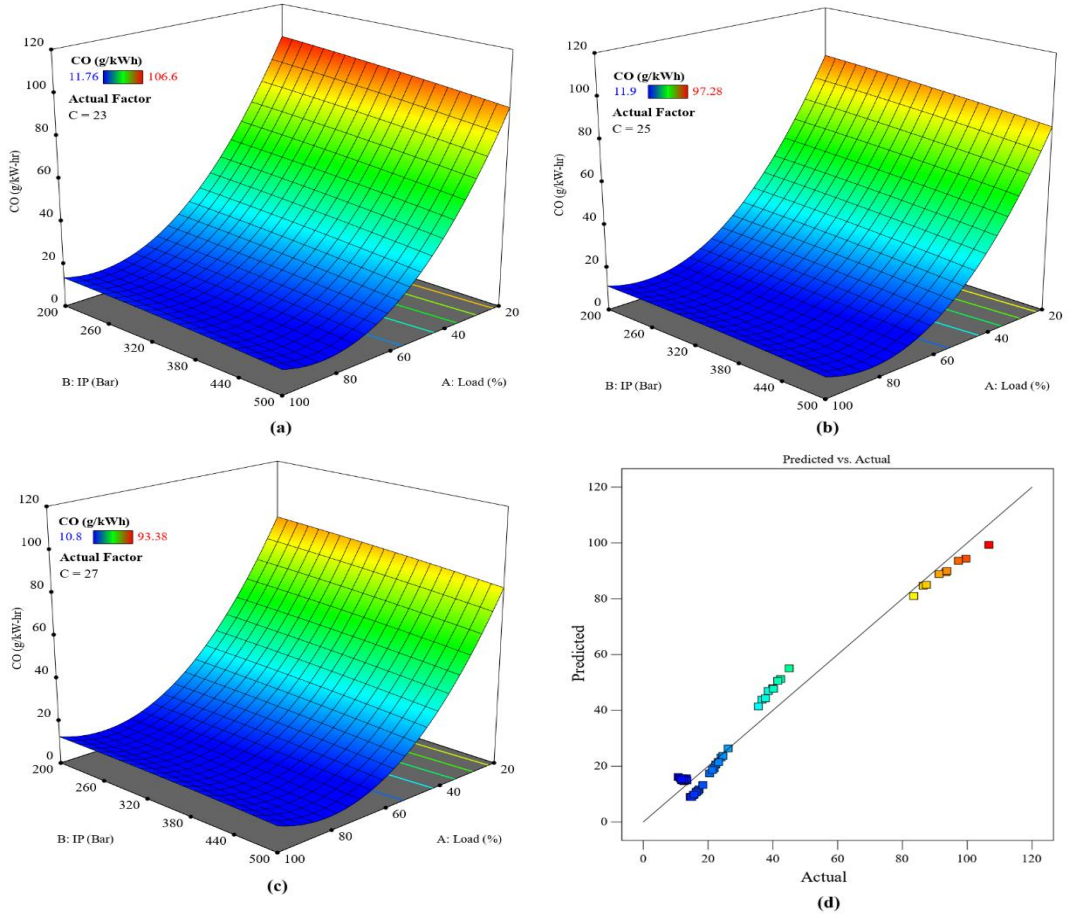

Figure 7. Effects CO with engine load for (a) FIT 23° CA (b) FIT 25° CA (c) FIT 27° CA (d) Predicted vs actual CO

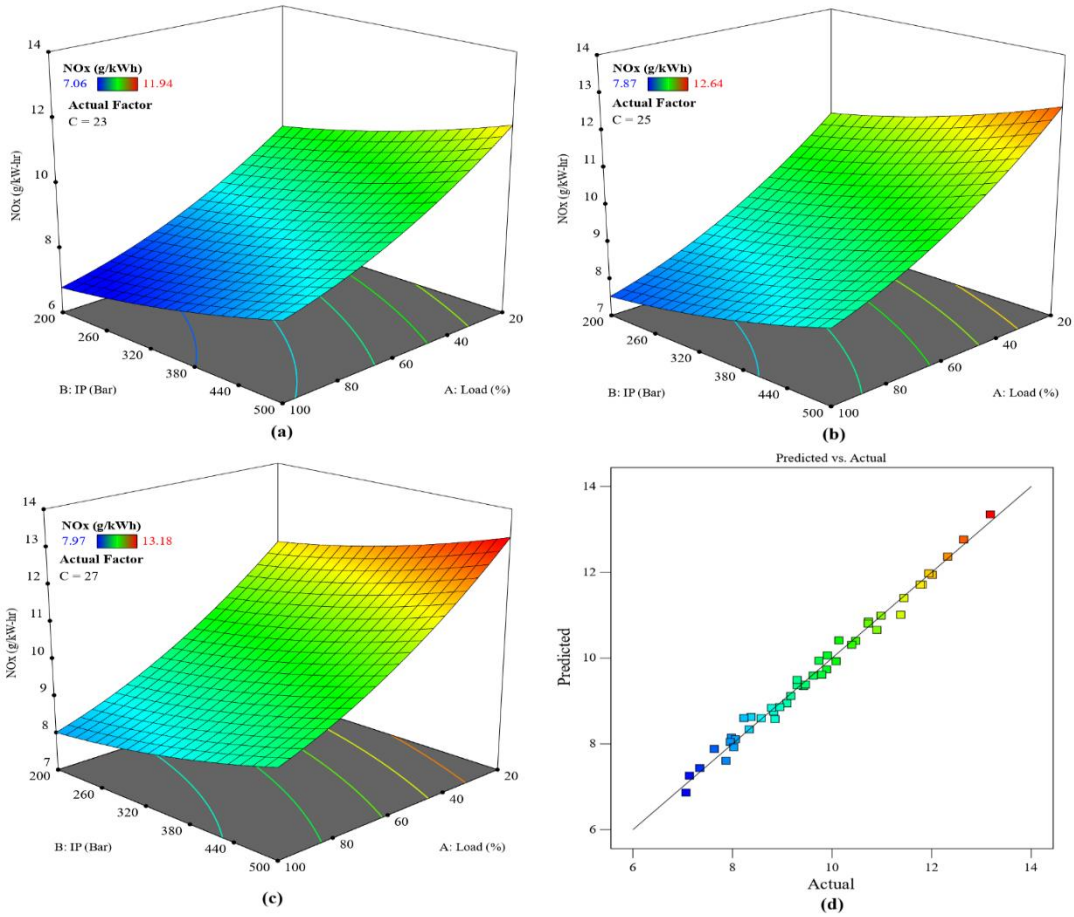

Figure 8. Effects NOx with engine load for (a) FIT 23° CA (b) FIT 25° CA (c) FIT 27° CA (d) Predicted vs actual NOx

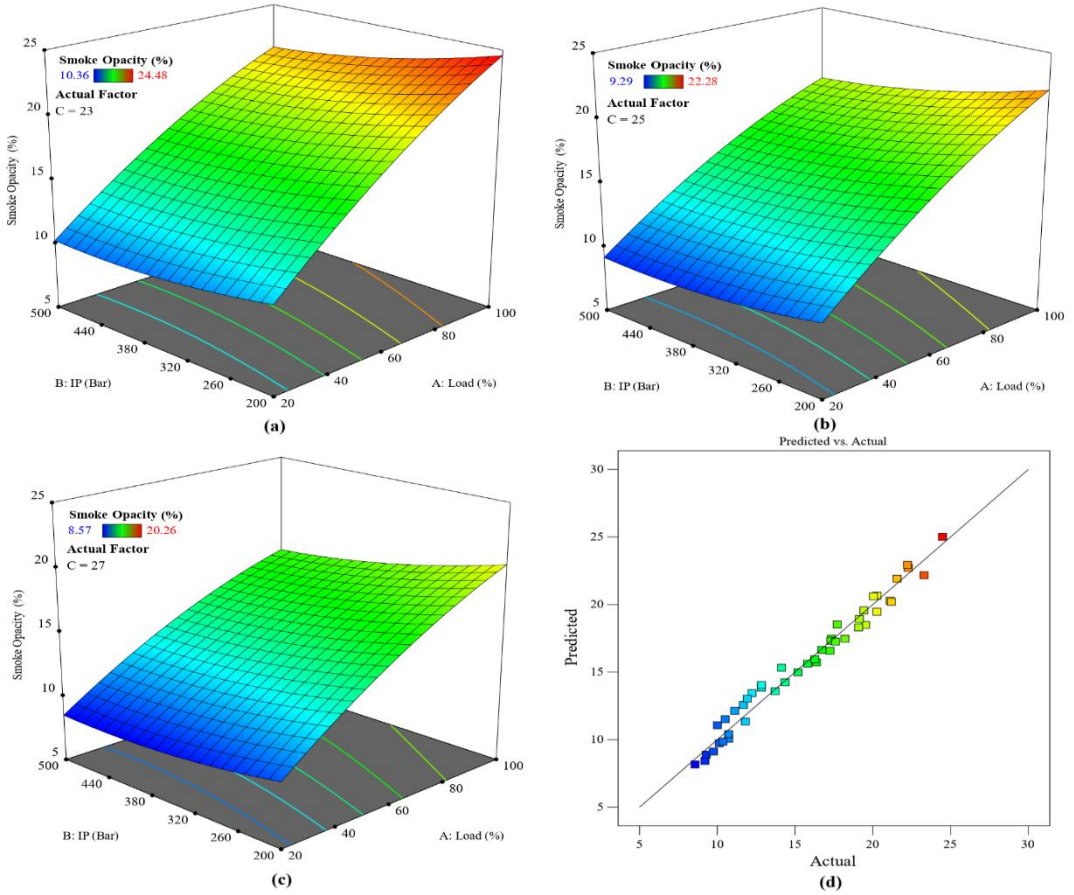

Figure 9. Effects Smoke with engine load for (a) FIT 23° CA (b) FIT 25° CA (c) FIT 27° CA (d) Predicted vs actual Smoke

Under peak load circumstances, the NOx emissions increased by 11-20% at 350 bar and by 16-25% at 500 bar when the injection time was 27°CA instead of the usual 23°CA and 25°CA. Increasing the injection timing lengthens the CD, which in turn keeps the burned gases in the combustion chamber for an extended period. This extended duration, combined with increased heat release rates, contributes to higher cylinder temperatures and elevated NOx emissions (Shameer & Ramesh 2018). With an injection time of 27°CA and an injection pressure of 500 bar, the HRR was determined to be highest, which contributed to the rise in NOx emissions.

3.2.4. Smoke emission of different FIT and FIP

The smoke emissions from WCO biofuel might vary depending on the injection pressure, time, and engine load, as shown in **Figure 9**. The data indicate that increasing the injection pressure slightly reduces smoke emissions across all load levels. At a typical injection timing of 23°CA and 100% load, the smoke emissions for WCO biofuel were 24.48% at 200 bar, 22.23% at 350 bar, and 21.56% at 500 bar. The oxygen in the WCO biofuel, together with better atomization at greater injection pressures, is responsible for this decrease (Aalam *et al.* 2016).

Higher injection pressures lead to smaller fuel droplet sizes, enhancing the air-fuel mixture and reducing smoke production during the injection process (Gumus *et al.* 2012). The **Figure 9** also demonstrates that advancing the injection timing significantly reduces smoke emissions. The smoke emissions for WCO biofuel at full load with injection pressures of 350 bar and 500 bar were 20.04% at 25°CA and 17.72% at 27°CA, respectively. At 25°CA, they dropped to 19.42% and 17.34% at 27°CA, respectively. The premixed combustion phase is mostly responsible for this decrease. A longer premixed combustion phase is achieved by increasing the injection time, which increases the quantity of fuel available at the start of combustion. More efficient combustion and reduced smoke emissions are the results of this prolonged phase's enhancement of the air-fuel mixture preparation during the ID (Gnanasekaran *et al.* 2016).

3.3. Optimization results of FIT and FIP of WCO combustion and its validation

Desirability acts as a quantitative measure, with values ranging from zero, indicating results outside acceptable limits, to one, representing achievement of the desired target. To find the optimal parameters for the desirability function, numerical optimization is used. When dealing with situations where there are several replies and outputs, the different goals of each response are combined into one desirability function. An important factor influencing the final desirable result is how close the specified minimum and maximum values are to the real ideal value.

Figure 10 shows that the overall desirability function achieves a peak value of 0.963 for the variables Load, FIT, and FIP. The predicted values for key output parameters ID, CD, BTE, BSFC, HC, CO, NOx, and smoke emissions are 14.61, 74.48, 27.91, 0.314, 3.217, 15.63, 8.203, and 18.841, respectively. This results in a desirability score of 0.983, indicating high reliability since the score is close to 1. To maximize BTE and decrease ID, CD, BSFC, HC, NOx, CO, and smoke emissions, precise parameter tuning is required for CI engines with appropriate FIT and FIP settings to achieve best performance. **Table 6** shows the experimental results, which show that no one configuration achieved all performance objectives at the same time. For instance, at full load, the best BTE was 31.18% at a FIT of 27° CA and a FIP of 350 pressure, but the best NOx emissions were 7.066 g/kWh at a FIT of 23° CA and a FIP of 200 bar. Other parameters achieved their optimal values under different conditions. Therefore, optimizing design parameters is critical to achieving a balanced trade-off among performance metrics.

An engine running on WCO combustion with specified FIT and FIP was able to attain a maximum BTE of 27.91%. At 14.61° CA, 74.48° CA, 0.314 kg/kWh, 3.217 g/kWh, 15.63 g/kWh, 8.203 g/kWh, and 18.84%, respectively, were the lowest recorded values for ID, CD, BTE, BSFC, HC, CO, and smoke emissions. These optimal outcomes were achieved at a FIT of 23° CA, an FIP of 350 bar, and an engine load of 70.13%.

The model achieved a desirability score of 0.963, indicating an effective balance across all performance parameters (Prasad *et al.* 2021). Experimental validation of these optimized design settings revealed a deviation of less than 5% between the predicted and observed results, confirming the model's accuracy. As shown in **Table 9**, the predicted optimal values closely align with experimental data. This demonstrates that the central composite design methodology is a dependable and efficient tool for optimizing WCO combustion in diverse CI engine setups.

3.4. Conclusion of modelling and optimization of FIP and FIT for WCO combustion

Many performance and emission characteristics were examined in this study, including ID, CD, BTE, BSFC, HC, CO, NOx, and Smoke, as well as the effects of the three main design elements Load, FIT, and FIP. Comparison of present work with existing research is listed in **Table 10**. The load, FIT, and FIP ranges that were investigated were 20-100%, 23° CA-27° CA, and 200-500 bar, respectively. Based on the optimization results, the optimal operating conditions for both performance and emissions were found to be FIT = 23° CA and FIP = 350 bar. The outcomes obtained are contrasted with the conventional mode running at 70% load listed in **Table 10**.

Table 9. Predicted optimal design factors alongside their experimental outcomes

Study	Load (%)	FIP (Bar)	FIT (CA)	ID (CA)	CD (CA)	BTE (%)	BSFC (kg/kWh)	CO (g/kWh))	HC (g/kWh))	NOx (g/kWh))	Smoke (%)
Mathematical	70.13	350	23	14.61	74.48	27.91	0.314	3.217	15.630	8.203	18.841
Experimental	70	350	23	15.5	76	27.45	0.327	3.36	16.13	8.51	19.52
% of error	0.19	0	0	5.74	2.00	1.65	3.98	4.26	3.10	3.61	3.48

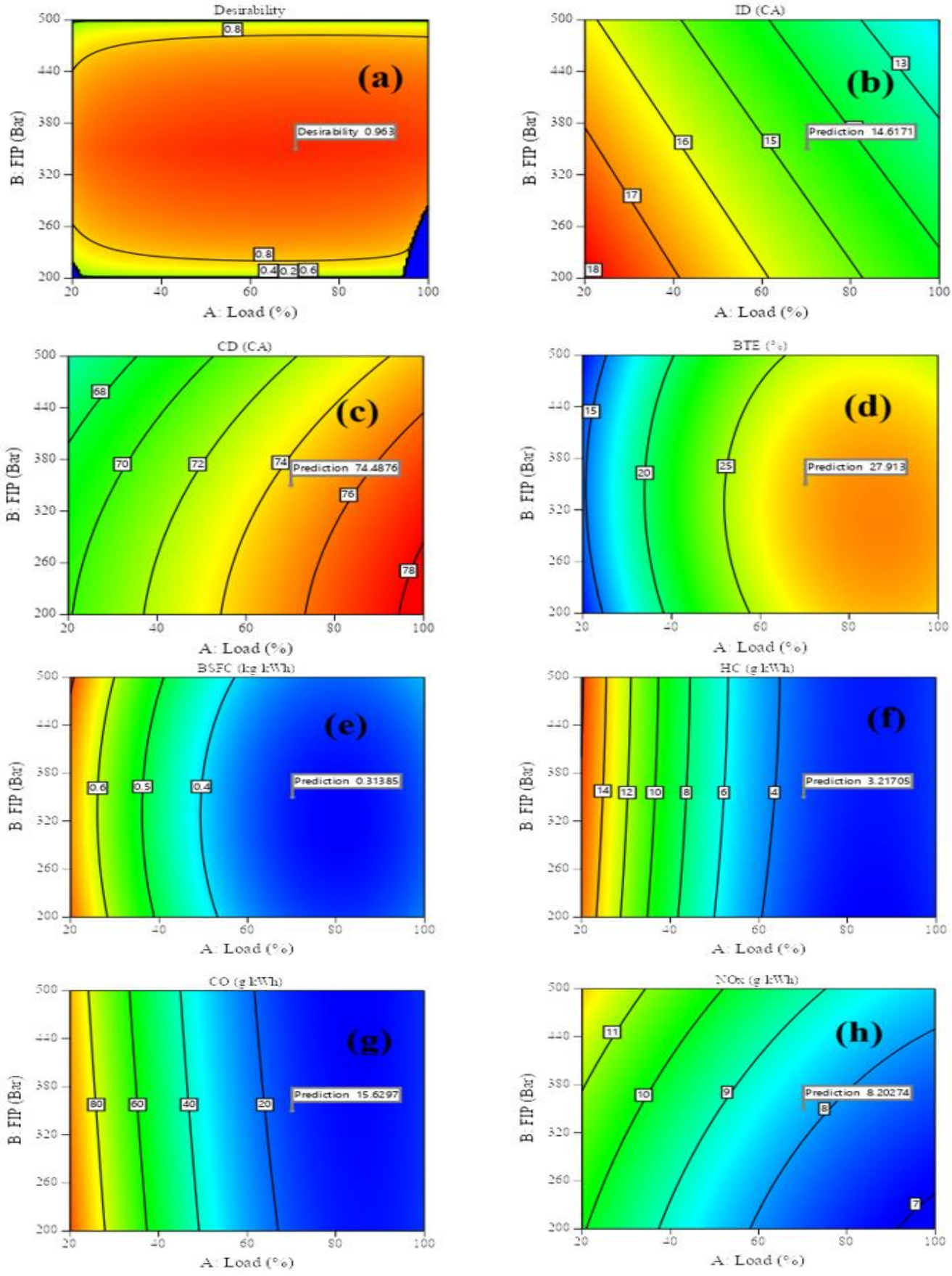

Figure 10. Desirability values on the FIP and FIP for WCO Combustion (a) Desirability (b) ID (c) CD (d) BTE (e) BSFC (f) HC (g) CO (h) NOx (i) Smoke

Table 10. Comparison of present work with existing research

Fuel type	Combustion type and Comparison	Engine Type	Combustion	Performance	Emission	Ref
Millettia pinnata (B100)	Compression Ignition & Diesel	4-Stroke, 1 Cyl, DI, 1500 rpm, 5kW	↑CP, ↓ID & CD	↓BSFC ↑BTE 34.6%	↓NOx ↑CO, HC	(Kalsi & Subramanian 2017)
CSO Blends (B10 to B30)	Compression Ignition & Diesel	4-Stroke, 1 Cyl, DI, 2300 rpm, 5.5kW, C_R - 18	-	↓BSFC 27% ↑BTE 36%	↓NOx 24% ↑HC, CO_2-17%	(Charitha *et al.* 2019)
Diesel & Methane	Compression Ignition & Diesel	4-Stroke, 1 Cyl, DI, 1500 rpm, 5kW, C_R – 12-19	↑CP	↓BSEC ↑BTE	↓NOx ↑CO, HC	(Armin & Gholinia 2022)
CSO biodiesel	Compression Ignition & Diesel	4-Stroke, 1 Cyl, DI, 1500 rpm, 5.4kW, C_R – 17.5	↓CP 5.1%, ↓HRR 3.7%	↓BSFC ↑2.4%	↓NOx 42.7% ↑CO 11.4% ↑HC 4.5%	(Ganesan, Le*, et al.* 2022)
Diesel & Isobutanol	Compression Ignition & Diesel	4-Stroke, 1 Cyl, DI, 1500 rpm, 4.4kW, C_R – 17.5, FIP – 220 bar	↓CP 4.3%, ↓HRR 4.1%	↓BSFC 4.3% ↑BTE 3.5%	↓NOx 57.5% ↑CO 13.1% ↑HC 6.5%	(Ganesh *et al.* 2019)
WCO biodiesel & Ethanol	Compression Ignition & Diesel	4-Stroke, 1 Cyl, DI, 1500 rpm, 3.7kW, C_R – 16, FIP – 200 bar	↓CP 3.1%, ↓HRR 4.7%	↓BSFC ↑BTE 6%	↓NOx% ↑CO 13.4% ↑HC 8.5%	(Guan *et al.* 2017)
WCO Biodiesel & LPG	Compression Ignition & Diesel	4-Stroke, 4 Cyl, DI, 3200 rpm, C_R – 19	↑CP 11.6%, ↑HRR 38.8%	↓BSFC ↓NOx 1.9% ↑CO 44.9% ↑HC 24.7%	↓NOx 1.9% ↑CO 44.9% ↑HC 24.7%	(Kumar *et al.* 2019)
WCO Biodiesel	Compression-Ignition & Diesel	4-Stroke, 1 Cyl, DI, 1500 rpm, 3.5kW	↓CP ↓HRR	↓BSFC ↑BTE 31.18%	↑NOx 2.14% ↓CO 12.2% ↓HC 1.29%	Present Work

Table 11. Desirability result

Number	Load	FIP	FIT	ID	CD	BTE	BSFC	HC	CO	NOx	Smoke	Desirability	
1	70.137	350.00	23.00	14.617	74.488	27.913	0.314	3.217	15.630	8.203	18.841	0.963	Selected
2	70.410	350.00	23.00	14.604	74.515	27.941	0.313	3.190	15.468	8.193	18.883	0.963	
3	70.039	350.00	23.00	14.622	74.477	27.903	0.314	3.227	15.688	8.206	18.826	0.963	
4	69.737	350.00	23.00	14.636	74.447	27.872	0.315	3.257	15.870	8.217	18.781	0.963	
5	70.838	349.99	23.00	14.584	74.559	27.983	0.312	3.149	15.222	8.178	18.947	0.963	

4. Conclusion

To learn more about the effects of varying the Fuel injection timing and pressure, WCO biodiesel experiments were conducted. A Compression ignition diesel engine was tested with WCO biodiesel combustion in this investigation and the main conclusions of the present investigation are listed below.

Experimental results revealed that variations in FIT and FIP with WCO biodiesel significantly improved engine performance. The highest BTE of 31.18% was achieved at an injection pressure of 350 bar and an advanced injection timing of 27° CA. Compared to a FIP of 350 bar and FIT of 23° CA, BTE increased by 2.93% and 12.21% at FIPs of 200 bar and 500 bar, respectively, with the same FIT at maximum load.

HC emissions were reduced by 1.29% and 6.5% at a FIP of 350 bar and 200 bar, respectively, compared to 500 bar, all with a FIT of 27° CA at maximum load.

CO emissions also showed significant reductions of 12.2% and 5.6% at FIPs of 350 bar and 500 bar, respectively, compared to 200 bar with the same FIT at maximum load.

However, NOx emissions increased with both advanced FIT and higher FIP under maximum load conditions. In contrast, smoke emissions decreased by 2.14% and 20.27% at FIPs of 350 bar and 500 bar, respectively, compared to 200 bar, all at a FIT of 27° CA.

These findings highlight the potential of optimizing FIT and FIP to enhance performance and reduce emissions when using WCO biodiesel. Optimization analysis revealed that the best performance and emission outcomes were achieved with a FIT of 23° CA and an FIP of 350 bar.

5. Limitations of this study and scope for future research

Overall, the study indicates that the optimization of fuel injection timing and fuel injection pressure of waste cooking oil biodiesel is a promising field of study with some

limitations. The study is limited in its ability to be applied to other contexts because of particular lab conditions, it ignores practical implementation complexities, it only provides a partial assessment of the environmental impact, and it fails to address long-term durability issues. In order to provide further insight into the viability of combustion with alternative fuels in practical applications, addressing these difficulties will increase its relevance. The potential for feature research can be focused on the reactivity-controlled compression ignition with multi-cylinder engines and engines operating at variable speeds, aiming to evaluate these parameters in diverse operational contexts.

References

Aalam, C.S., Saravanan, C. and Anand, B.P. (2016), Impact of high fuel injection pressure on the characteristics of CRDI diesel engine powered by mahua methyl ester blend, *Applied Thermal Engineering*, **106**, 702–711.

Agarwal, A.K., Dhar, A., Gupta, J.G., Kim, W.I., Choi, K., Lee, C.S. and Park, S. (2015). Effect of fuel injection pressure and injection timing of Karanja biodiesel blends on fuel spray, engine performance, emissions and combustion characteristics, *Energy Conversion Management*, **91**, 302–314.

Akash, D., Sarbjot Singh, S. and Subhash, C. (2017). Experimental investigations on the influence of fuel injection timing and pressure on single cylinder C.I. engine fueled with 20% blend of castor biodiesel in diesel, *Fuel*, **210**, 15–22.

Armin, M. and Gholinia, M. (2022). Comparative evaluation of energy, performance, and emission characteristics in dual-fuel (CH4/Diesel) heavy-duty engine with RCCI combustion mode, *Results in Engineering*, **16**, 100766.

Arunprasad, S. and Balusamy, T. (2018). Experimental investigation on the performance and emission characteristics of a diesel engine by varying the injection pressure and injection timing using mixed biodiesel, *International Journal of Green Energy*, **15**(6), 376–384.

Ashok, B., Nanthagopal, K., Raj, R.T.K., Bhasker, J.P. and Vignesh, D.S. (2017). Influence of injection timing and exhaust gas recirculation of a Calophyllum inophyllum methyl ester fuelled CI engine, *Fuel Processing Technology*, **167**, 18–30.

Bragadeshwaran, A., Rajasekar, V., Usman, K.M., Ayyasamy, T. and Govindasamy, K. (2023). Split injection strategy control map development through prediction-based calibration approach to improve the biodiesel-fuelled diesel engine characteristics, *Environmental Science Pollution Research*, 1–25.

Charitha, V., Thirumalini, S., Prasad, M. and Srihari, S. (2019). Investigation on performance and emissions of RCCI dual fuel combustion on diesel-bio diesel in a light duty engine, *Renewable Energy*, **134**, 1081–1088.

Dey, S., Reang, N.M., Das, P.K. and Deb, M. (2021). Comparative study using RSM and ANN modelling for performance-emission prediction of CI engine fuelled with bio-diesohol blends: A fuzzy optimization approach, *Fuel*, **292**, 120356.

Ganesan, N., Le, T.H., Ekambaram, P., Balasubramanian, D. and Hoang, A.T. (2022). Experimental assessment on performance and combustion behaviors of reactivity-controlled compression ignition engine operated by n-pentanol and cottonseed biodiesel, *Journal of Cleaner Production*, **330**, 129781.

Ganesan, N., Viswanathan, K., Karthic, S., Ekambaram, P., Wu, W. and Vo, D.-V.N. (2022). Split injection strategies based RCCI combustion analysis with waste cooking oil biofuel and methanol in an open ECU assisted CRDI engine, *Fuel*, **319**, 123710.

Ganesh, D., Ayyappan, P. and Murugan, R. (2019). Experimental investigation of iso-butanol/diesel reactivity controlled compression ignition combustion in a non-road diesel engine, *Applied Energy*, **242**, 1307–1319.

Gnanasekaran, S., Saravanan, N. and Ilangkumaran, M. (2016). Influence of injection timing on performance, emission and combustion characteristics of a DI diesel engine running on fish oil biodiesel, *Energy*, **116**, 1218–1229.

Guan, C., Cheung, C.S., Ning, Z., Wong, P.K. and Huang, Z. (2017). Comparison on the effect of using diesel fuel and waste cooking oil biodiesel as pilot fuels on the combustion, performance and emissions of a LPG-fumigated compression-ignition engine, *Applied Thermal Engineering*, **125**, 1260–1271.

Gültekin, N. (2024a). Experimental study of the effects of diesel, bioethanol, and hydrogen on combustion, emissions, mechanical vibration, and noise in a CI engine with different valve lift, *International Journal of Hydrogen Energy*, **93**, 1011–1021.

Gültekin, N. (2024b). The hydrogen injection strategy's influence on the performance and emissions (exhaust, vibration, and noise) of a dual-fuel engine, *International Journal of Automotive Engineering Technologies*, **13**(4), 217–229.

Gültekin, N. and Ciniviz, M. (2023). Experimental investigation of the effect of hydrogen ratio on engine performance and emissions in a compression ignition single cylinder engine with electronically controlled hydrogen-diesel dual fuel system, *International Journal of Hydrogen Energy*, **48**(66), 25984–25999.

Gültekin, N. and Ciniviz, M. (2024). Investigation of the effect of advance angle on performance and emissions (exhaust, vibration, noise) in a single-cylinder diesel engine whose fuel system is converted to common rail, *Environmental Progress & Sustainable Energy Technologies and Assessments*, **43**(1), 14261.

Gumus, M., Sayin, C. and Canakci, M. (2012). The impact of fuel injection pressure on the exhaust emissions of a direct injection diesel engine fueled with biodiesel–diesel fuel blends, *Fuel*, **95**, 486–494.

Hirkude, J.B. and Padalkar, A.S. (2014). Performance optimization of CI engine fuelled with waste fried oil methyl ester-diesel blend using response surface methodology, *Fuel*, 119, 266–273.

Kalsi, S.S. and Subramanian, K. (2017). Experimental investigations of effects of hydrogen blended CNG on performance, combustion and emissions characteristics of a biodiesel fueled reactivity controlled compression ignition engine (RCCI), *International Journal of Hydrogen Energy*, **42**(7), 4548–4560.

Kannan, G.R. and Anand, R. (2012). Effect of injection pressure and injection timing on DI diesel engine fuelled with biodiesel from waste cooking oil, *Biomass and Bioenergy*, **46**, 343–352.

Kumar, A., Pali, H.S. and Kumar, M. (2024). Effective utilization of waste plastic derived fuel in CI engine using multi objective optimization through RSM, *Fuel*, **355**, 129448.

Kumar, A.N., Kishore, P., Raju, K.B., Nanthagopal, K. and Ashok, B. (2020). xperimental study on engine parameters variation in CRDI engine fuelled with palm biodiesel, *Fuel*, **276**, 118076.

Kumar, M.S., Arul, K. and Sasikumar, N. (2019). Impact of oxygen enrichment on the engine's performance, emission and combustion behavior of a biofuel based reactivity controlled compression ignition engine, *Journal of the Energy Institute*, **92**(1), 51–61.

Kumar, S. and Pal, A. (2022). Multi-objective-parametric optimization of diesel engine powered with fuel additive 2-ethylhexyl nitrate-algal biodiesel, *Sustainable Energy Technologies and Assessments*, **53**, 102518.

Li, Z., Wang, Y., Geng, H., Zhen, X., Liu, M., Xu, S. and Li, C. (2019). Parametric study of a diesel engine fueled with directly injected methanol and pilot diesel, *Fuel*, **256**, 115882.

Li, Z., Wang, Y., Geng, H., Zhen, X., Liu, M., Xu, S. and Li, C. (2020). Investigation of injection strategy for a diesel engine with directly injected methanol and pilot diesel at medium load, *Fuel*, **266**, 116958.

Maurya, R.K. and Agarwal, A.K. (2014). Experimental investigations of performance, combustion and emission characteristics of ethanol and methanol fueled HCCI engine, *Fuel Processing Technology*, **126**, 30–48.

Naik, B.D., Meivelu, U., Thangarasu, V., Annamalai, S. and Sivasankaralingam, V. (2022). Experimental and empirical analysis of a diesel engine fuelled with ternary blends of diesel, waste cooking sunflower oil biodiesel and diethyl ether, *Fuel*, **320**, 123961.

Nirmala, N., Dawn, S. and Harindra, C. (2020). Analysis of performance and emission characteristics of Waste cooking oil and Chlorella variabilis MK039712. 1 biodiesel blends in a single cylinder, four strokes diesel engine, *Renewable Energy*, **147**, 284–292.

Prabu, S.S., Asokan, M., Roy, R., Francis, S. and Sreelekh, M. (2017). Performance, combustion and emission characteristics of diesel engine fuelled with waste cooking oil bio-diesel/diesel blends with additives, *Energy*, **122**, 638–648.

Prasad, G.A., Murugan, P., Wincy, W.B. and Sekhar, S.J. (2021). Response Surface Methodology to predict the performance and emission characteristics of gas-diesel engine working on producer gases of non-uniform calorific values, *Energy*, **234**, 121225.

Puhan, S., Jegan, R., Balasubbramanian, K. and Nagarajan, G. (2009). Effect of injection pressure on performance, emission and combustion characteristics of high linolenic linseed oil methyl ester in a DI diesel engine, *Renewable Energy*, **34**(5), 1227–1233.

Saravanan, C., Kiran, K.R., Vikneswaran, M., Rajakrishnamoorthy, P. and Yadav, S.P.R. (2020). Impact of fuel injection pressure on the engine characteristics of CRDI engine powered by pine oil biodiesel blend, *Fuel*, **264**, 116760.

Sathish Kumar, T., Ashok, B., Senthil Kumar, M., Vignesh, R., Saiteja, P., Ramachandra Bhat Hire, K., Ayyasamy, T. (2022). Biofuel powered engine characteristics improvement through split injection parameter multivariate optimization with titanium based nano-particle additives, *Fuel*, **322**, 124178.

Sathiskumar, S. and Priyanka, E. (2024). Enhancing reactivity-controlled compression ignition engine performance: A response surface methodology approach with ammonium hydroxide-waste cooking oil biodiesel optimization, *Proceedings of the Institution of Mechanical Engineers, Part E: Journal of Process Mechanical Engineering*.

Shameer, P.M. and Ramesh, K. (2018). Assessment on the consequences of injection timing and injection pressure on combustion characteristics of sustainable biodiesel fuelled engine, *Renewable Sustainable Energy Reviews*, **81**, 45–61.

Sharma, A. and Murugan, S. (2016). Experimental evaluation of combustion parameters of a DI diesel engine operating with biodiesel blend at varying injection timings. In 169, *Proceedings of the First International Conference on Recent Advances in Bioenergy Research*,

Sharma, A. and Murugan, S. (2017). Effect of nozzle opening pressure on the behaviour of a diesel engine running with non-petroleum fuel, *Energy*, **127**, 236–246.

Tamilvanan, A., Balamurugan, K., Ashok, B., Selvakumar, P., Dhamotharan, S., Bharathiraja, M. and Karthickeyan, V. (2020). Effect of diethyl ether and ethanol as an oxygenated additive on Calophyllum inophyllum biodiesel in CI engine, *Environmental Science and Pollution Research*, 28(26), 33880–33898.

Tamilvanan, A., Mohanraj, T., Ashok, B. and Santhoshkumar, A. (2023). Enhancement of energy conversion and emission reduction of Calophyllum inophyllum biodiesel in diesel engine using reactivity controlled compression ignition strategy and TOPSIS optimization, *Energy*, **264**, 126168.

Wang, S., Karthickeyan, V., Sivakumar, E. and Lakshmikandan, M. (2020). Experimental investigation on pumpkin seed oil methyl ester blend in diesel engine with various injection pressure, injection timing and compression ratio, *Fuel*, **264**, 116868.

Yaashikaa, P.R., Keerthana Devi, M., Senthil Kumar, P. and Pandian, E. (2022). A review on biodiesel production by algal biomass: Outlook on lifecycle assessment and techno-economic analysis, *Fuel*, **324**, 124774.